Acta Crystallographica Section F
Structural Biology and Crystallization Communications
ISSN 1744-3091

Cloning, purification, crystallization and preliminary X-ray diffraction analysis of mouse PACSIN 3 protein

Xiaoyun Bai,[a,b] Geng Meng[a,b] and Xiaofeng Zheng[a,b]*

[a]State Key Laboratory of Protein and Plant Gene Research, School of Life Sciences, Peking University, Beijing 100871, People's Republic of China, and [b]Department of Biochemistry and Molecular Biology, School of Life Sciences, Peking University, Beijing 100871, People's Republic of China

Correspondence e-mail: xiaofengz@pku.edu.cn

Received 12 August 2011
Accepted 17 November 2011

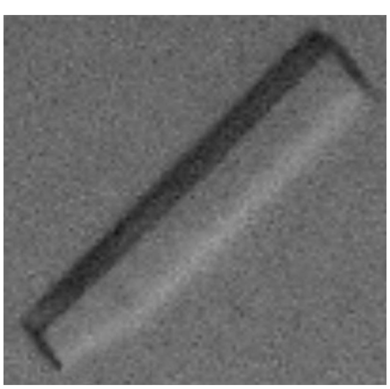

PACSIN-family proteins are cytoplasmic proteins that have vesicle-transport, membrane-dynamics, actin-reorganization and microtubule activities. Here, the N-terminal F-BAR domain of mouse PACSIN 3, which contains 341 amino acids, was successfully cloned, purified and crystallized. The crystal of PACSIN 3 (1–341) diffracted to 2.6 Å resolution and belonged to space group $P2_1$, with unit-cell parameters $a = 46.9$, $b = 54.7$, $c = 193.7$ Å, $\alpha = 90$, $\beta = 96.9$, $\gamma = 90°$. These data should provide further information on PACSIN-family protein structures.

1. Introduction

BAR-domain proteins function in various membrane-remodelling processes such as vesicle budding, cell division and membrane trafficking (Gallop *et al.*, 2006; Bhatia *et al.*, 2009; Masuda *et al.*, 2006; Takei *et al.*, 1999; Farsad *et al.*, 2001; Mattila *et al.*, 2007). These proteins can deform membranes into tubules *via* their banana-like dimer concave surface (Peter *et al.*, 2004), and the diameter of the tubules matches the curvature of the dimer concave surface (Itoh *et al.*, 2005; Gallop *et al.*, 2006; Heath & Insall, 2008; Masuda *et al.*, 2006). There are three distinct families of BAR-domain proteins: N-BAR (N-terminal amphipathic helix BAR), F-BAR (EFC/F-BAR, Fes/CIP4 homology BAR) and I-BAR (inverse-BAR). In comparison to N-BAR and I-BAR proteins, F-BAR proteins possess a distinctly shallower curvature and normally generate low-curvature membrane tubules (Itoh *et al.*, 2005; Fütterer & Machesky, 2007; Shimada *et al.*, 2007; Henne *et al.*, 2007; Masuda *et al.*, 2006; Peter *et al.*, 2004).

PACSINs, which are a branch of the F-BAR-domain protein family, are cytoplasmic proteins that function in vesicle transport, endocytosis (Damke *et al.*, 1994; Hinshaw & Schmid, 1995; Takei *et al.*, 1995, 1999) and actin reorganization and as components of the centrosome involved in microtubule dynamics (Modregger *et al.*, 2000; Qualmann & Kelly, 2000; Braun *et al.*, 2005; Kessels *et al.*, 2006; Grimm-Günter *et al.*, 2008). The PACSIN-family proteins consist of three isoforms: neurospecific PACSIN 1, the ubiquitously expressed PACSIN 2, and PACSIN 3, which is primarily found in lung and muscle tissues (Plomann *et al.*, 1998; Qualmann *et al.*, 1999; Ritter *et al.*, 1999; Modregger *et al.*, 2000). PACSINs 1 and 2 share a conserved structure that contains an N-terminal α-helical region, a C-terminal Src homology 3 (SH3) domain and potential asparagine–proline–phenylalanine (NPF) motif(s) that are essential for binding to Eps15 homology domain proteins (Paoluzi *et al.*, 1998; Modregger *et al.*, 2000). The three-dimensional structures of the F-BAR domains of PACSINs 1 and 2 from human, mouse and *Drosophila* have previously been reported (Wang *et al.*, 2009; Rao *et al.*, 2010; Plomann *et al.*, 2010; Edeling *et al.*, 2009) and revealed that the F-BAR domains of PACSINs 1 and 2 share a conserved helix-bundle structure with a unique wedge loop. However, the structure of PACSIN 3 has not been reported to date.

PACSIN 3 differs from PACSIN 1 and PACSIN 2 in containing a short multi-proline region and in lacking the NPF motifs (Modregger *et al.*, 2000). Human and mouse PACSIN 3 encode 424 amino acids and have high sequence identity (Sumoy *et al.*, 2001). Amino-acid sequence alignment reveals that the F-BAR domain of mouse PACSIN 3 shares 55 and 60% sequence identity with those of mouse PACSINs 1 and 2, respectively (Fig. 1). PACSIN 3 shows different functions in cells compared with PACSINs 1 and 2 (Sumoy *et al.*, 2001; Cuajungco *et al.*, 2006; Modregger *et al.*, 2000). Overexpression of PACSIN 3 can increase transport of adipocyte glucose in the clathrin-coated pit pathway (Roach & Plomann, 2007). It has been demonstrated that PACSIN 3 specifically affects the endocytosis of TRPV4 and subsequently regulates the subcellular localization of TRPV4 (Cuajungco *et al.*, 2006). A recent study showed that PACSIN 3 influences the columnar organization of the notochord during early development in zebrafish (Edeling *et al.*, 2009). Therefore, structure determination of the F-BAR domain of PACSIN 3 will help us to further understand its functions.

Here, we expressed, purified and crystallized mouse PACSIN 3 F-BAR domain (1–341). Preliminary X-ray diffraction analysis of this protein should provide us with further information on PACSIN-family protein structures and help us to understand the molecular mechanism of how PACSIN proteins work in their related activities.

2. Methods and results

2.1. Cloning and protein expression

PACSIN 3 (1–341) was amplified by polymerase chain reaction (PCR) using the cDNA of mouse *pacsin 3* (a gift from Professor Plomann) as a template. The PCR product was digested with *Bam*HI and *Hin*dIII and then cloned into the same restriction-enzyme sites of a pET28a vector. The resulted plasmid was confirmed by DNA sequencing and then transformed into *Escherichia coli* strain BL21 (DE3) and plated onto a Luria–Bertani broth (LB) agar plate containing 100 mg $^{-1}$ kanamycin. Cells from a single clone were grown

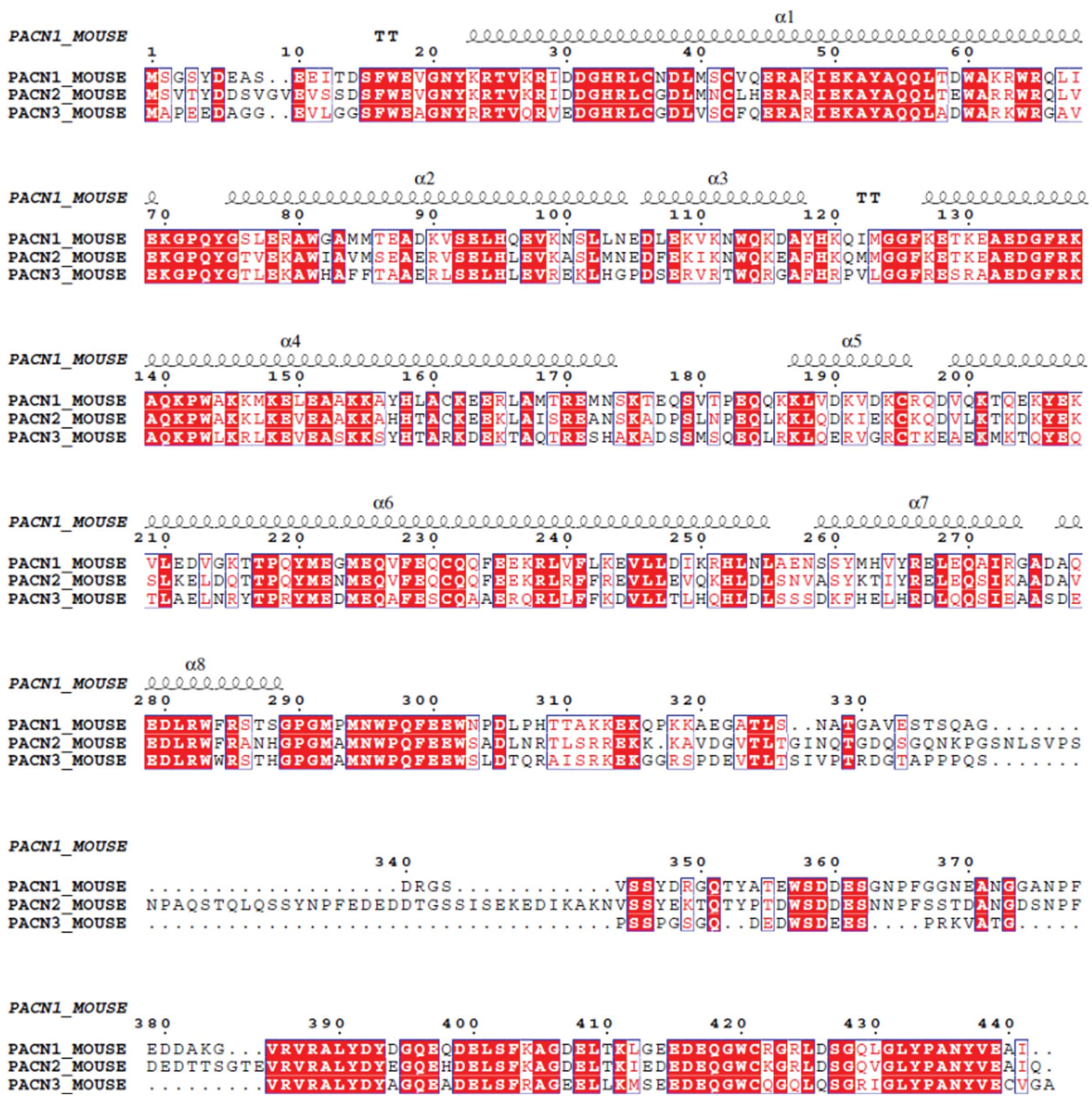

Figure 1

Amino-acid sequence alignment of mouse PACSINs. Sequence alignment was performed using *ClustalX* and *ESPript* (Gouet *et al.*, 1999). The secondary structure of PACSIN 1 is shown at the top: α-helices are displayed as squiggles and β-turns as TT. Strictly conserved residues are shown in white lettering on a red background. Similar residues are indicated in red.

overnight at 310 K in LB medium until the OD_{600} reached 0.6; 0.5 m*M* isopropyl β-D-1-thiogalactopyranoside (IPTG) was then added and culture continued for a further 6 h at 303 K. Cells were harvested by centrifugation at 5000 rev min $^{-1}$ for 10 min at 277 K and frozen at 193 K.

2.2. Protein purification

The cells were resuspended in binding buffer consisting of 50 m*M* HEPES pH 7.5, 500 m*M* NaCl and 5 m*M* imidazole and then sonicated. The lysate was centrifuged at 18 000 rev min^{-1} for 30 min at 277 K. The supernatant was filtered through a 0.22 µm filter and applied onto a 5 ml Ni^{2+} HiTrap affinity column (GE Healthcare, USA). The Ni^{2+} HiTrap affinity column was washed with 15 column volumes of binding buffer to remove nonspecifically bound proteins and PACSIN 3 was eluted in binding buffer containing 500 m*M* imidazole. Finally, peak fractions of PACSIN 3 (1–341) were pooled, concentrated to 2 ml and further purified on a Superdex 75 gel-filtration column (GE Healthcare) equilibrated in 500 m*M* NaCl, 10 m*M* HEPES pH 7.5. The final yield of purified protein was 5 mg per litre of culture, with a purity of 95% (Fig. 2).

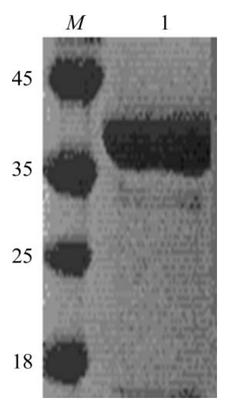

Figure 2
SDS–PAGE analysis of purified PACSIN 3 (1–341). *M*, marker (labelled in kDa); lane 1, purified PACSIN 3 (1–341) after a two-step purification.

Table 1
Crystallographic parameters and data-collection statistics for PACSIN 3.

Values in parentheses are for the last shell.

Wavelength (Å)	0.97924
Resolution (Å)	30–2.6 (2.67–2.60)
Completeness (%)	95.2 (75.1)
R_{merge}† (%)	5.6 (30.2)
$\langle I/\sigma(I)\rangle$	35.4 (3.4)
Space group	$P2_1$
Unit-cell parameters (Å)	a = 46.9, b = 54.7, c = 193.7
No. of observed reflections	133167
No. of unique reflections	28175
Molecules in asymmetric unit	2
V_M ($Å^3$ Da^{-1})	3.33
Solvent content (%)	63.04

† $R_{merge} = \sum_{hkl}\sum_i |I_i(hkl) - \langle I(hkl)\rangle| / \sum_{hkl}\sum_i I_i(hkl)$.

2.3. Crystallization

The purified protein was concentrated to 10 mg ml^{-1} for crystallization. Initial crystallization experiments were performed at 293 K by the sitting-drop vapour-diffusion method in 96-well plates using the PEG/Ion, Crystal Screen, Crystal Screen 2 and Index kits from Hampton Research. Each droplet consisted of 1 µl protein solution and 1 µl reservoir solution and was equilibrated against 150 µl reservoir solution as previously reported (Bai *et al.*, 2010).

Crystals were obtained under the condition 200 m*M* potassium thiocyanate, 20% PEG 3350 pH 7.0 (Fig. 3*a*). Further crystal optimization was improved by fine-tuning the pH in the range 5.0–9.0 (in 0.1 pH-unit increments) and adding different additives (5% glycerol, 10 m*M* $CaCl_2$, 10 m*M* $MgCl_2$ or 1% ethanol). After crystal optimization, better diffracting crystals were obtained using 200 m*M* potassium thiocyanate, 100 m*M* HEPES pH 7.3, 100 m*M* $CaCl_2$, 20%(*w*/*v*) PEG 3350 at 293 K within one week (Fig. 3*b*).

2.4. Diffraction data collection

For data collection, crystals were soaked in cryoprotectant solution supplemented with 30%(*v*/*v*) glycerol. The crystal was mounted in a large cryoloop and flash-cooled at 100 K in a nitrogen stream. The crystal-to-detector distance was 300 mm. X-ray diffraction data were collected using a MAR 345 image-plate detector on beamline 3W1A at Beijing Synchrotron Radiation Facility. A total of 500 frames of

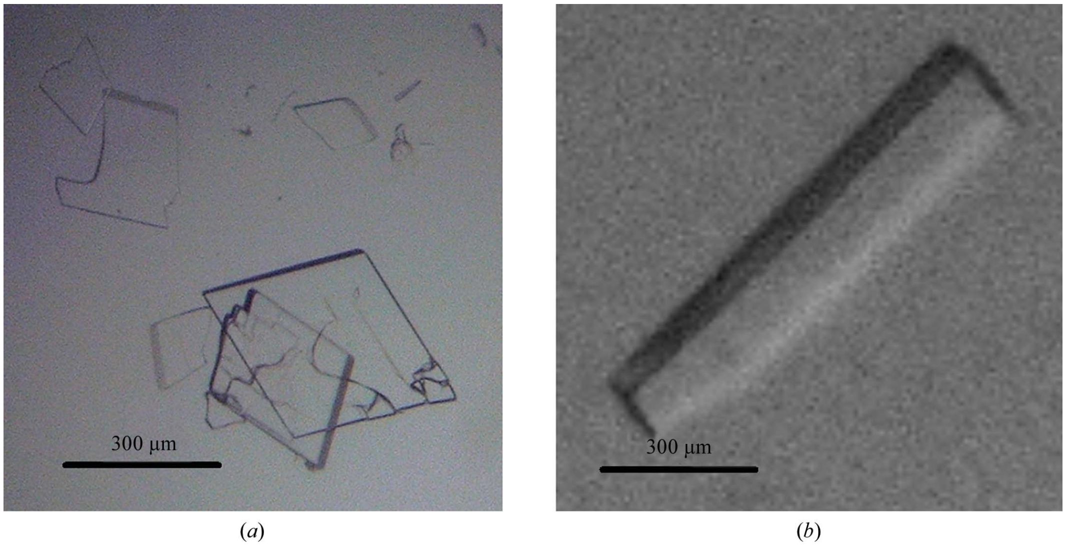

(*a*) (*b*)

Figure 3
(*a*) Initial crystals of PACSIN 3 (1–341). (*b*) Optimized crystal of PACSIN 3 (1–341).

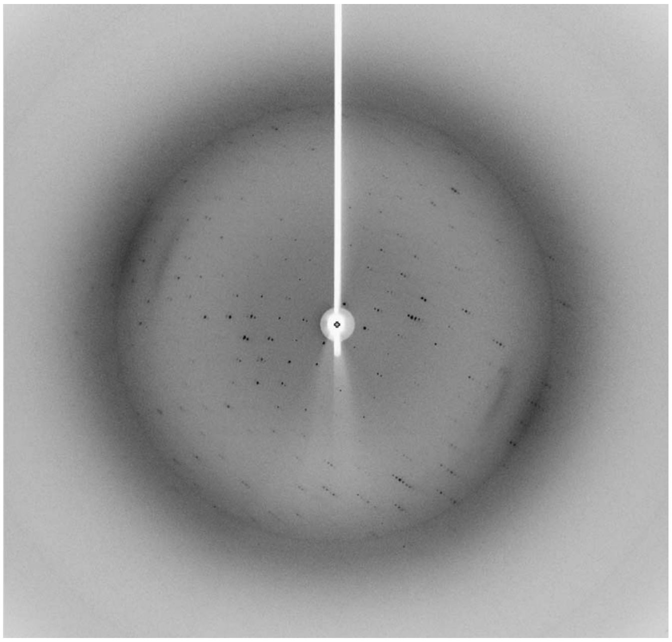

Figure 4
Diffraction pattern of the PACSIN 3 (1–341) crystal.

0.5° oscillation were measured with 10 s exposure per frame. All data were processed with *HKL*-2000 (Otwinowski & Minor, 1997).

The crystal of mouse PACSIN 3 (1–341) diffracted to 2.6 Å resolution (Fig. 4). The crystal belonged to space group $P2_1$, with unit-cell parameters $a = 46.9$, $b = 54.7$, $c = 193.7$ Å, $\alpha = 90$, $\beta = 96.9$, $\gamma = 90°$. The unit-cell parameters are consistent with the presence of two molecules in the asymmetric unit. Data-collection statistics are given in Table 1.

We thank Dr Plomann at Stanford University School of Medicine for providing us with the PACSIN 3 plasmid. X-ray diffraction data collection was carried out at the Beijing Synchrotron Radiation Laboratory, Institute of High Energy Physics, Chinese Academy of Sciences. This work was supported by grants from the National High Technology and Development Program of China (973 Program; Nos. 2010CB911800 and 2007CB914303) and the International Centre for Genetic Engineering and Biotechnology (ICGEB; Project No. CRP/CHN09-01).

References

Bai, X., Meng, G., Li, G., Luo, M. & Zheng, X. (2010). *Acta Cryst.* F**66**, 73–75.

Bhatia, V. K., Madsen, K. L., Bolinger, P. Y., Kunding, A., Hedegård, P., Gether, U. & Stamou, D. (2009). *EMBO J.* **28**, 3303–3314.

Braun, A., Pinyol, R., Dahlhaus, R., Koch, D., Fonarev, P., Grant, B. D., Kessels, M. M. & Qualmann, B. (2005). *Mol. Biol. Cell*, **16**, 3642–3658.

Cuajungco, M. P., Grimm, C., Oshima, K., D'hoedt, D., Nilius, B., Mensenkamp, A. R., Bindels, R. J., Plomann, M. & Heller, S. (2006). *J. Biol. Chem.* **281**, 18753–18762.

Damke, H., Baba, T., Warnock, D. E. & Schmid, S. L. (1994). *J. Cell Biol.* **127**, 915–934.

Edeling, M. A., Sanker, S., Shima, T., Umasankar, P. K., Honing, S., Kim, H. Y., Davidson, L. A., Watkins, S. C., Tsang, M., Owen, D. J. & Traub, L. M. (2009). *PLoS One*, **4**, e8150.

Farsad, K., Ringstad, N., Takei, K., Floyd, S. R., Rose, K. & De Camilli, P. (2001). *J. Cell Biol.* **155**, 193–200.

Fütterer, K. & Machesky, L. M. (2007). *Cell*, **129**, 655–657.

Gallop, J. L., Jao, C. C., Kent, H. M., Butler, P. J., Evans, P. R., Langen, R. & McMahon, H. T. (2006). *EMBO J.* **25**, 2898–2910.

Gouet, P., Courcelle, E., Stuart, D. I. & Métoz, F. (1999). *Bioinformatics*, **15**, 305–308.

Grimm-Günter, E. M., Milbrandt, M., Merkl, B., Paulsson, M. & Plomann, M. (2008). *Exp. Cell Res.* **314**, 1991–2003.

Heath, R. J. & Insall, R. H. (2008). *J. Cell Sci.* **121**, 1951–1954.

Henne, W. M., Kent, H. M., Ford, M. G., Hegde, B. G., Daumke, O., Butler, P. J., Mittal, R., Langen, R., Evans, P. R. & McMahon, H. T. (2007). *Structure*, **15**, 839–852.

Hinshaw, J. E. & Schmid, S. L. (1995). *Nature (London)*, **374**, 190–192.

Itoh, T., Erdmann, K. S., Roux, A., Habermann, B., Werner, H. & De Camilli, P. (2005). *Dev. Cell*, **9**, 791–804.

Kessels, M. M., Dong, J., Leibig, W., Westermann, P. & Qualmann, B. (2006). *J. Cell Sci.* **119**, 1504–1516.

Masuda, M., Takeda, S., Sone, M., Ohki, T., Mori, H., Kamioka, Y. & Mochizuki, N. (2006). *EMBO J.* **25**, 2889–2897.

Mattila, P. K., Pykäläinen, A., Saarikangas, J., Paavilainen, V. O., Vihinen, H., Jokitalo, E. & Lappalainen, P. (2007). *J. Cell Biol.* **176**, 953–964.

Modregger, J., Ritter, B., Witter, B., Paulsson, M. & Plomann, M. (2000). *J. Cell Sci.* **113**, 4511–4521.

Otwinowski, Z. & Minor, W. (1997). *Methods Enzymol.* **276**, 307–326.

Paoluzi, S., Castagnoli, L., Lauro, I., Salcini, A. E., Coda, L., Fre', S., Confalonieri, S., Pelicci, P. G., Di Fiore, P. P. & Cesareni, G. (1998). *EMBO J.* **17**, 6541–6550.

Peter, B. J., Kent, H. M., Mills, I. G., Vallis, Y., Butler, P. J., Evans, P. R. & McMahon, H. T. (2004). *Science*, **303**, 495–499.

Plomann, M., Lange, R., Vopper, G., Cremer, H., Heinlein, U. A., Scheff, S., Baldwin, S. A., Leitges, M., Cramer, M., Paulsson, M. & Barthels, D. (1998). *Eur. J. Biochem.* **256**, 201–211.

Plomann, M., Wittmann, J. G. & Rudolph, M. G. (2010). *J. Mol. Biol.* **400**, 129–136.

Qualmann, B. & Kelly, R. B. (2000). *J. Cell Biol.* **148**, 1047–1062.

Qualmann, B., Roos, J., DiGregorio, P. J. & Kelly, R. B. (1999). *Mol. Biol. Cell*, **10**, 501–513.

Rao, Y., Ma, Q., Vahedi-Faridi, A., Sundborger, A., Pechstein, A., Puchkov, D., Luo, L., Shupliakov, O., Saenger, W. & Haucke, V. (2010). *Proc. Natl Acad. Sci. USA*, **107**, 8213–8218.

Ritter, B., Modregger, J., Paulsson, M. & Plomann, M. (1999). *FEBS Lett.* **454**, 356–362.

Roach, W. & Plomann, M. (2007). *Biochem. Biophys. Res. Commun.* **355**, 745–750.

Shimada, A. *et al.* (2007). *Cell*, **129**, 761–772.

Sumoy, L., Pluvinet, R., Andreu, N., Estivill, X. & Escarceller, M. (2001). *Gene*, **262**, 199–205.

Takei, Y., Harada, A., Takeda, S., Kobayashi, K., Terada, S., Noda, T., Takahashi, T. & Hirokawa, N. (1995). *J. Cell Biol.* **131**, 1789–1800.

Takei, K., Slepnev, V. I., Haucke, V. & De Camilli, P. (1999). *Nature Cell Biol.* **1**, 33–39.

Wang, Q., Navarro, M. V., Peng, G., Molinelli, E., Goh, S. L., Judson, B. L., Rajashankar, K. R. & Sondermann, H. (2009). *Proc. Natl Acad. Sci. USA*, **106**, 12700–12705.